



**Discover Generics**

Cost-Effective CT & MRI Contrast Agents

 **FRESENIUS  
KABI**

[WATCH VIDEO](#)

**AJNR**

**Pathophysiology of Acute Intracerebral and  
Subarachnoid Hemorrhage: Applications to MR  
Imaging**

L. Anne Hayman, John J. Pagani, Joel B. Kirkpatrick and Vincent  
C. Hinck

This information is current as  
of June 24, 2025.

*AJNR Am J Neuroradiol* 1989, 10 (3) 457-461  
<http://www.ajnr.org/content/10/3/457>

# Pathophysiology of Acute Intracerebral and Subarachnoid Hemorrhage: Applications to MR Imaging

L. Anne Hayman<sup>1</sup>  
John J. Pagani<sup>2</sup>  
Joel B. Kirkpatrick<sup>3</sup>  
Vincent C. Hinck<sup>1</sup>

In this review of the pathophysiology of acute intracerebral and subarachnoid hemorrhage, information from several disciplines is assembled to describe the bleeding process, hemostasis and coagulation, fibrinolysis, erythrocyte lysis, phagocytosis, and changes in the state of hemoglobin. The impact of these pathophysiologic processes upon MR imaging, CT, and angiography is noted.

There are significant gaps in knowledge and unresolved controversies concerning the physical and biochemical changes that occur in intracranial hemorrhage. Prior to the advent of MR imaging, there was little need for this information. This article is designed primarily to assemble information concerning the pathophysiology of acute (0–10 days) intracerebral and subarachnoid hemorrhage in an attempt to unify theories, focus research efforts, and assist in the interpretation of clinical images.

Because a recent review has chronicled the sequential MR imaging changes in intracranial hemorrhage [1], only brief reference will be made here to current MR imaging theories. Instead, attention will be focused on the bleeding process, hemostasis and coagulation, including clot matrix formation and changes in hematocrit, cell lysis, phagocytosis, fibrinolysis, and the state of the hemoglobin molecule. Many of these changes have not been evaluated quantitatively so their relative effects on MR cannot be assessed. Further, some pathophysiologic changes have been included that may have as yet undiscovered significant MR properties. The article is divided into two sections: intracerebral and subarachnoid hemorrhage, respectively.

## Intracerebral Hemorrhage

### *Origin and Duration of Bleeding*

Cerebral angiography has demonstrated that intracerebral hemorrhage usually originates from a single artery or arterialized vein. It may continue for many hours or days. In one study of hypertensive arterial hemorrhage, bleeding could be demonstrated angiographically in almost one-half (five of 12) of the patients examined within 5 hr of the onset of symptoms [2]. Less vigorous bleeding would be occult arteriographically, but is probably a common and significant event nonetheless.

Serial histologic sections of intracerebral hematomas demonstrate that hemorrhage occurs not only at the primary angiographically detected arterial site(s) but also from torn arterioles at the margin of the expanding hematoma [3] (Fig. 1A). These are secondary bleeding sites and are created as blood dissects along white matter fiber tracts. They have been identified angiographically at the periphery of intracerebral hematomas as late as 16 and 20 days after clinical onset [4]. It is clear, therefore, that intracerebral hematomas are typically heterogeneous, slowly expanding collections of blood.

This article appears in the May/June 1989 issue of *AJNR* and the July 1989 issue of *AJR*.

Received October 21, 1988; accepted December 5, 1988.

<sup>1</sup> Department of Radiology, Baylor College of Medicine, One Baylor Plaza, Houston, TX 77030. Address reprint requests to L. A. Hayman.

<sup>2</sup> Department of Radiology, AMI Park Plaza Hospital, Houston, TX 77030.

<sup>3</sup> Department of Pathology, Baylor College of Medicine, Houston, TX 77030.

*AJNR* 10:457–461, May/June 1989  
0195–6108/89/1003–0457

© American Society of Neuroradiology

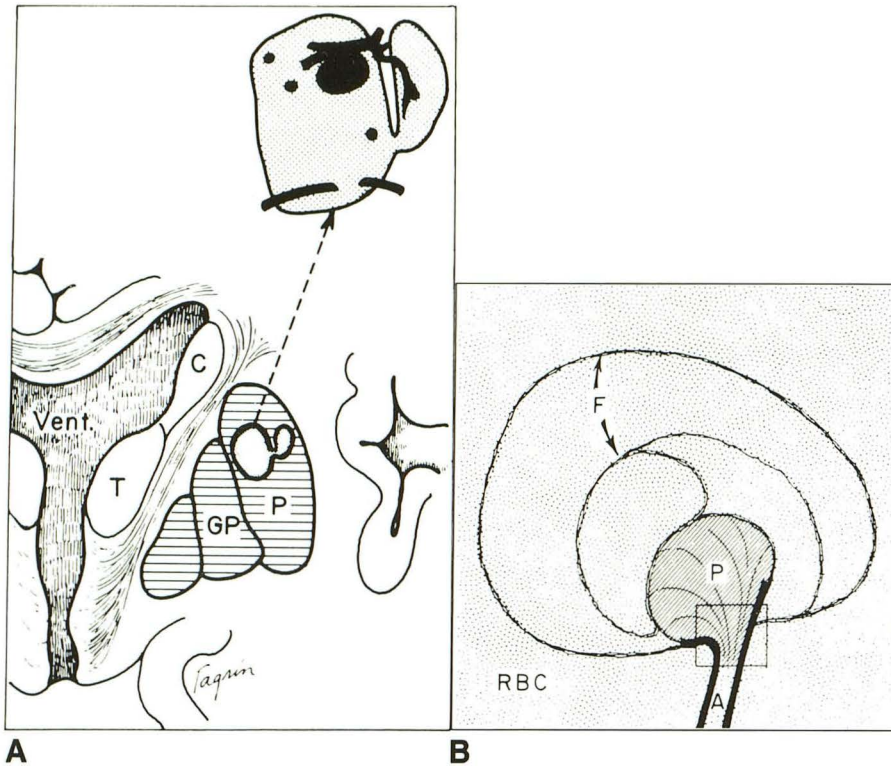


Fig. 1.—A, Coronal schematic of microscopically studied putaminal hemorrhage. Enlarged drawing of hemorrhage demonstrates RBC mass (*inset*), fibrin globes (one large and three small round black areas within *inset*), and disrupted arterioles (horizontal black bars within *inset*). Note similarity to CT images of the actively bleeding hypertensive hematoma shown in Fig. 3. Vent. = ventricles, T = thalamus, C = caudate, GP = globus pallidus, P = putamen.

B, Schematic of the larger (5-mm) "fibrin globe" (seen in the enlargement in A) identified microscopically within an intracerebral hemorrhage. A = ruptured artery; RBC = mass of red blood cells within and around the fibrin globes (F); P = platelet mass. (Both schematics reprinted with permission from [3].)

When the brain can no longer compensate for expanding hematoma, neurologic symptoms evolve. Assumptions that bleeding begins at the onset of these clinical symptoms and that bleeding ceases prior to an MR imaging examination are unfounded. It is unfortunate that these assumptions are often inherent in the conclusions reached in many clinical MR series evaluating acute intracranial bleeding. This may be one of the reasons why MR imaging patterns show considerable variation among clinically similar subjects.

#### Hemostasis and Coagulation

Erythrocyte aggregation begins within seconds after blood extravasates into the brain [5]. The MR properties associated with the membrane-membrane interactions that are responsible for erythrocyte aggregation are unknown. This subject requires investigation.

Within minutes after normal blood has extravasated into tissue, two important concomitant clotting processes begin. The first establishes hemostasis by forming a platelet plug(s) at the bleeding point(s). The second process is a sequential, highly ordered and complex series of plasma-protein interactions that employ the intrinsic and extrinsic clotting pathways [6]. Thrombin formation converts fibrinogen to fibrin, which subsequently assembles into a highly ordered, polymeric, unretracted fibrin clot. Initially, this clot is held together by electrostatic interactions between neighboring fibrin monomers. Stabilization of the clot is achieved eventually by covalent cross-linkages between adjacent fibrin molecules [6]. In our laboratory, we have noted that the formation of this unretracted clot *in vitro* causes a mild T2 shortening on MR images [Hayman LA, Taber KH, Ford JJ. Role of clot formation in MR of blood (in preparation)]. Subsequent clot retraction

occurs *if* platelets are functioning normally. *In vitro*, this process is nearly complete within 4 hr and has a significant T2 shortening effect. In general, clot retraction produces an inhomogeneous packing of the blood cells interspersed with macroscopic zones of fibrin. This appearance can be demonstrated in the *in vitro* acute blood clot shown in Figure 2.

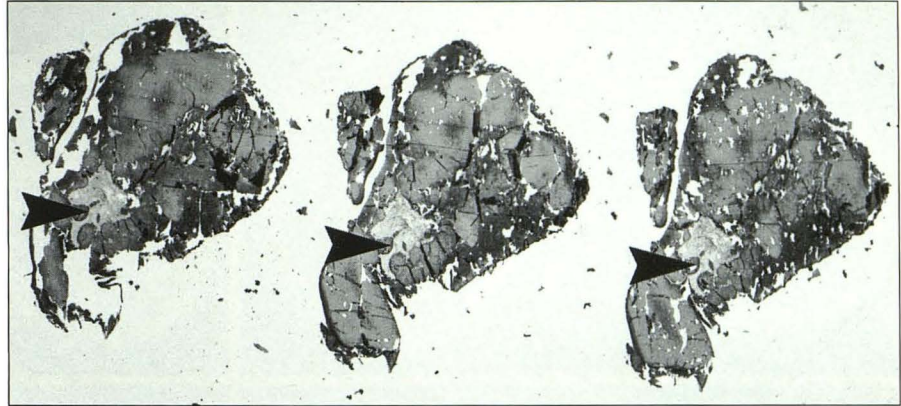
Microscopic examination of an *in vivo* clot demonstrates an internal architecture around the point(s) of hemorrhage. Multiple fibrin strands form concentric, three-dimensional shells, which surround the bleeding site. These have been termed "fibrin globes," "bleeding globes" [3], or "pseudoaneurysms" [7] (Fig. 1B). Within each is a fine fibrin mesh that contains zones of tightly packed erythrocytes interspersed with small platelet clumps. These globes appear to confine successive waves of extravasated blood. On contrast-enhanced CT scans of established acute hematoma, the contrast-laden, freshly extravasated blood is seen to accumulate within this fibrin network (Fig. 3).

The formation of a stable retracted clot packs the cells to a hematocrit of approximately 70–90% [Hayman (in preparation) and 8]. Much of the serum is retained to a great extent within the clot matrix. Some of it forms a thin band of "acellular, proteinaceous liquid" surrounding acute (1–3 days) intracerebral hematomas [9, 10].

The fibrinolytic system, driven by the conversion of plasminogen to plasmin, may be operative even in this early period. It is responsible for removing the fibrin globes and meshwork that originally formed in the clot [6]. The MR effects of this process are unknown.

A wide variety of commonly encountered diseases and medications are known to alter the scenario of blood clot formation described above. For example, high blood alcohol

Fig. 2.—Serial 5- $\mu$ m sections of an in vitro blood clot demonstrate the inhomogeneous clumping of red cells and a large zone of fibrin (arrowheads). Multiple smaller strands of fibrin separate the densely packed, deformed erythrocytes. At higher magnification, these small strands can be seen as they pass in and out of the plane of section.



levels, often found in association with traumatic intracerebral hemorrhage, will enhance the development of intracranial hematoma by disturbing the function of platelets, coagulation, and membrane-bound enzymes [11]. Chronic liver disease can alter blood coagulation. Bleeding disorders, which affect the ability of platelets to seal leaking vessels, can be caused by chemotherapy or aspirin, which alters the number and/or function of platelets. Any of these conditions may, therefore, alter the MR appearance of hemorrhage. Failure to include information relative to the bleeding or clotting conditions in the analysis of clinical MR imaging studies of intracerebral hemorrhage may, therefore, preclude accurate interpretation of the data.

#### *Changes in Cellular Morphology and Distribution*

After hemorrhage occurs, erythrocytes within the hematoma retain their normal biconcave configuration for a while. However, by day 4, in an experimental model of hemorrhage, they become amorphous and, as a result, more tightly packed [9]. Initial red cell lysis occurs at the center of the hematoma. It can be seen after 4–8 days in the canine hemorrhage model [9] and after 5–10 days in a human autopsy series of premature infant and adult brains [12]. Minimal peripheral red cell lysis may be seen in this period [12]. This finding contradicts the current theory that attributes MR signal changes in the periphery of subacute hematoma to initial peripheral, not central, cell lysis [8].

#### *Changes in Hemoglobin Oxygen State*

Initially, densely packed intact erythrocytes within a hematoma contain a mixture of oxyhemoglobin ( $O_2Hb$ ), deoxyhemoglobin (Hb), and methemoglobin (MHb), which is usually identical to that of arterial blood. As the concentration of paramagnetic Hb and MHb within the hematoma changes, the MR signal pattern should change [13]. The rate of change and the number of factors responsible for these changes in hemoglobin oxygenation are unknown. Some of the factors that may be responsible are discussed below.

Erythrocyte metabolism depends on the availability of glucose from the surrounding plasma. The erythrocyte has no

glycogen stores. If the cells become glucose-deprived, there will be a corresponding decrease in, and ultimate failure of, normal erythrocyte metabolic function, membrane integrity, and activity of the enzyme systems, which prevent the conversion of  $O_2Hb$  to Hb and MHb [14].

Current theories, evoked to explain the MR appearance of blood, postulate that, within 24–72 hr of hemorrhage, intracerebral hematomas contain intact erythrocytes with high concentrations of intracellular Hb [8]. To confirm this, it will be necessary to analyze erythrocyte integrity as well as  $O_2Hb$ , Hb, MHb, glucose, and other parameters in samples obtained intraoperatively from human hematomas.

#### **Subarachnoid Hemorrhage**

Immediately after hemorrhage, the subarachnoid space is filled with erythrocytes suspended in the CSF. These erythrocytes may follow one of several pathways. Some will be trapped within the clot that forms at the bleeding site. The majority will be trapped within the arachnoid villi and trabeculae [15]. These are rapidly cleared from the CSF into the vascular system. Fifty percent of the trapped cells will be removed by day 1 and 90% within 1 week [16].

Red cells are also removed from the subarachnoid space by phagocytosis [15]. This process begins within 24 hr after hemorrhage. CSF macrophages, which arise from the arachnoid mesothelial cells or enter the subarachnoid space via the meningeal vessels, may directly ingest erythrocytes suspended in CSF or those within a blood clot. These become hemosiderin-laden macrophages and are eventually removed. If chronic, recurrent subarachnoid hemorrhages occur, they may accumulate in the leptomeninges, subpial tissue and/or the surface of the spinal cord, cranial nerves, or ventricular ependyma.

Lysis of the suspended erythrocytes is another mechanism that can remove blood cells from the CSF. It begins within hours after subarachnoid hemorrhage and peaks 5–7 days later [16]. Lysis releases  $O_2Hb$  and smaller amounts of Hb, iron, heme pigments, and MHb into the CSF. The  $O_2Hb$  is degraded to bilirubin and other metabolic by-products by the enzyme heme-oxygenase, which is present in mesothelial arachnoid lining cells, choroid plexus, and circulating CSF macrophages [16]. Heme-oxygenase activity in the CSF in-

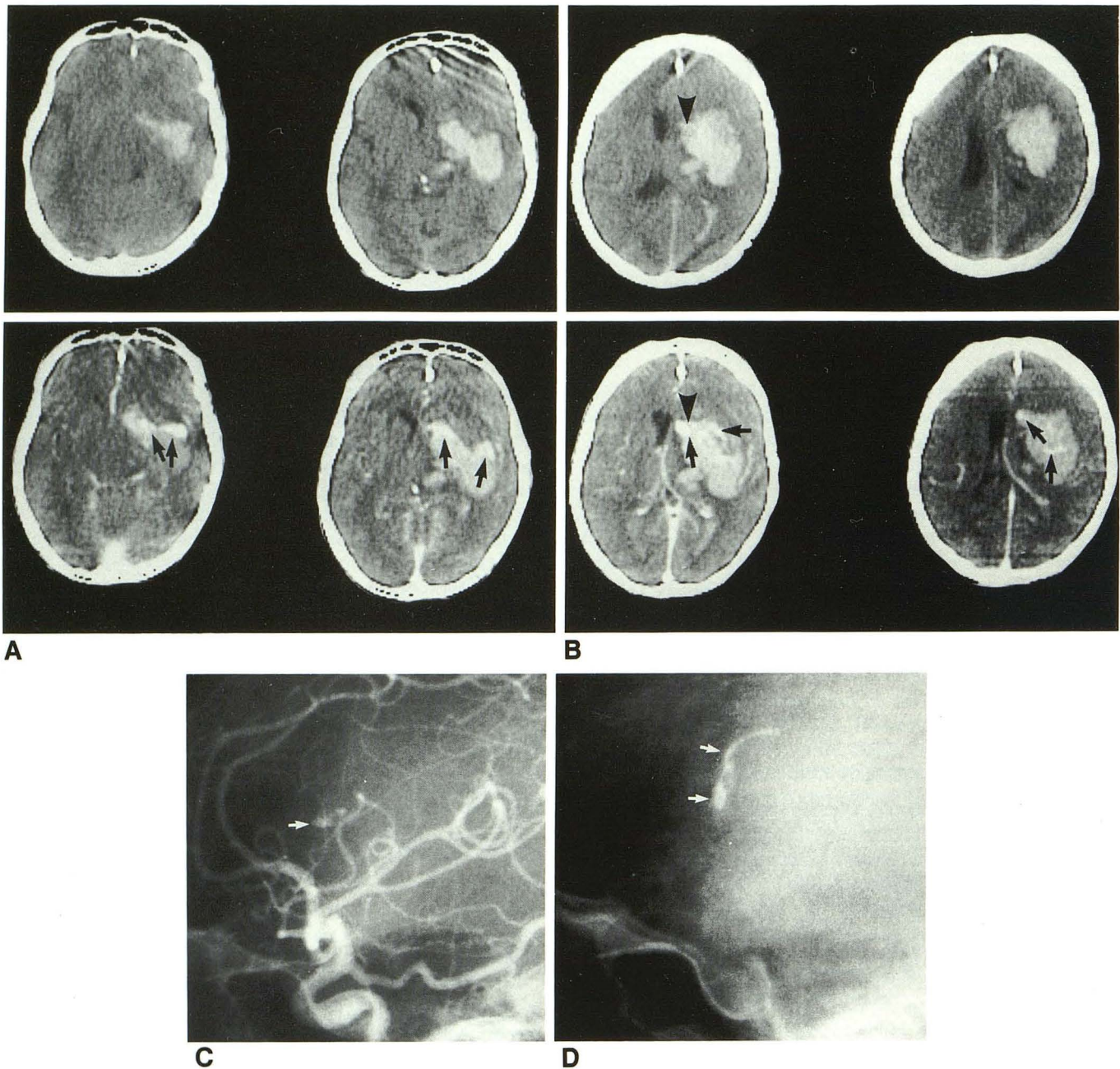


Fig. 3.—A and B, Precontrast CT scans of acute hypertensive hematoma (upper row). Companion CT scans obtained immediately after contrast enhancement (lower row) show extravasation of contrast medium at multiple bleeding sites. (Some of these are indicated by arrows.) Note that fibrin network forms sharply defined margins, which compartmentalize the freshly extravasated contrast-laden blood. Arrowheads mark surface of hyperdense, settled blood cells at a lenticulostriate bleeding point.

C and D, Selective left lateral carotid angiograms done immediately after CT show extravasation of contrast medium (arrows) in arterial and late venous phases, respectively.

creases rapidly after hemorrhage, peaks within 2–3 days, and then gradually declines. The earliest activity of this enzyme produces early peak CSF bilirubin levels, which slowly decrease over a period of 1–2 weeks. As the activity of hemoxygenase declines, a gradual elevation of extracellular  $O_2Hb$  occurs. A very small amount of this  $O_2Hb$  is converted into extracellular MHb [17]. The highest reported CSF MHb level that we have been able to identify in the clinical literature was negligible at days 0–7 and less than 75 mg/100 ml CSF at 11 days after clinical onset [17]. The latter was noted in a case

of massive subarachnoid hemorrhage that cleared from the CSF very slowly. These extremely low levels of MHb raise some doubts that the reported T1 shortening observed in clinically subacute, subarachnoid hemorrhage is due to these minute changes in the CSF concentration of MHb [18].

Lysis of the fibrin structure in a subarachnoid blood clot is presumably accelerated because of the fibrinolytic nature of the CSF. (This has been a point of contention in the literature.) However, it has been shown that fibrinolytic activators are present in small meningeal and cerebral arteries and in the

choroid plexus [19]. The activity of these agents is thought to explain why so few cisternal subarachnoid clots lead to obstructive hydrocephalus.

In summary, a large body of knowledge regarding the morphologic and biochemical features of acute intracerebral and subarachnoid hemorrhage has been reviewed. The many gaps in our knowledge of these subjects have been noted, and the effects that these pathophysiologic features have on CT and current MR imaging theories have been discussed.

#### REFERENCES

- Bradley WG. MRI of hemorrhage and iron in the brain. In: Stark DD, Bradley WG, eds. *Magnetic resonance imaging*. St. Louis: Mosby, **1988**:359–374
- Yamaguchi K, Uemura K, Takahashi H, Kowada M, Takashi K. Intracerebral leakage of contrast medium in apoplexy. *Br J Radiol* **1971**;44:689–691
- Fisher CM. Pathological observations in hypertensive cerebral hemorrhage. *J Neuropathol Exp Neurol* **1971**;30:536–549
- Bergstrom K, Lodin H. An angiographic observation in intracerebral haematoma. *Br J Radiol* **1967**;40:228–229
- Lillihei KO, Chandler WF, Knake JE. Real time ultrasound characteristics of acute intracerebral hemorrhage as studied in the canine model. *Neurosurgery* **1984**;14:48–51
- Miller JR. Blood coagulation and fibrinolysis. In: Nelson DA, Henry JB, eds. *Clinical diagnosis and management by laboratory methods*. Philadelphia: Saunders, **1984**:765–789
- Zimmerman RA, Bilaniuk LT. Computed tomographic staging of traumatic epidural bleeding. *Radiology* **1982**;144:809–812
- Gomori JM, Grossman RI, Goldberg HI, Zimmerman RA, Bilaniuk LT. Intracranial hematomas: Imaging by high-field MR. *Radiology* **1985**;157:87–93
- Enzmann DR, Britt RH, Lyons BE, Buxton JL, Wilson DA. Natural history of experimental intracerebral hemorrhage: sonography, computed tomography, and neuropathology. *AJNR* **1981**;2:517–526
- Takasugi S, Ueda S, Matsumoto K. Chronological changes in spontaneous intracerebral hematoma—an experimental and clinical study. *Stroke* **1985**;16:651–658
- Cowan DH. The platelet defect in alcoholism. *Ann NY Acad Sci* **1975**;157:252–328
- Darrow VC, Alvord EC, Mack LA, Hodson WA. Histologic evolution of the reactions to hemorrhage in the premature human infant's brain. *Am J Pathol* **1988**;130:44–58
- Weingarten K, Zimmerman RD, Markisz J, Cahill P, Sze G, Deck MDF. The effect of hemoglobin oxygenation on the MR intensity of experimentally produced intracranial hematomas at 0.6 T and 1.5 T. *AJNR* **1988**;9:1015 (abstr)
- Yoshikawa H, Rapoport SM. *Cellular and molecular biology of erythrocytes*. Baltimore: University Park, **1974**
- Laurent JP. Computed tomographic scanning in subarachnoid hemorrhage. In: Wood JH, ed. *Neurobiology of cerebrospinal fluid*. New York: Plenum, **1980**:283–284
- Wahlgren NG, Lindquist C. Haem derivatives in the cerebrospinal fluid after intracranial haemorrhage. *Eur Neurol* **1987**;26:216–221
- Tourtellotte WW, Metz LN, Bryan ER, DeJong RN. Spontaneous subarachnoid hemorrhage. *Neurology* **1964**;14:301–306
- Bradley WG, Schmidt PG. Effect of methemoglobin formation on the MR appearance of subarachnoid hemorrhage. *Radiology* **1985**;156:99–103
- Vecht J. Haemostatic function in haemostasis in acute neurological disorders. Assen/Amsterdam: Van Gorcum, **1975**:3–11